Mechanisms Underlying the Hyperexcitability of CA3 and Dentate Gyrus Hippocampal Neurons Derived From Bipolar Disorder Patients

Supplemental Information

Supplemental Methods

Patients

As previously described, all participants underwent diagnostic assessments that followed a strict procedure; after signing an informed consent, they were interviewed by pairs of experienced clinician researchers blind to the subject status.

Cell culture: DG neurons

Briefly, iPSC colonies were grown in TeSR and lifted using collagenase to form embryoid bodies (EBs). After 2 days, medium was replaced with anti-caudalizing (AC) medium in a base of DMEM/F12 with Glutamax and N2 and B27 (minus vitamin A) with Human Noggin 0.5 ug/ml, DKK1 0.5 ug/ml, Cyclopamine 1μM, and SB431542 10 μM. EBs were fed with AC medium until Day 20. On day 20 EBs were plated on laminin/polyornithine-coated plates to form neural rosettes. Rosettes were manually picked and dissociated on day 27 using accutase and replated on laminin/polyornithine-coated plates to form neural progenitor cells (NPCs). Cells were fed with N2B27 medium with 20 ng/ml FGF2 and 1ug/ml Laminin. When NPCs cultures were confluent, cells were dissociated again and plated on laminin/polyornithine-coated coverslips. One day after replating, neural differentiation medium was used to culture the cells containing DMEM/B12 with Glutamax and N2 and B27 (minus vitamin A) with added ascorbic acid (200 nM), cyclic AMP (cAMP; 500 mg/ml), laminin (1 mg/ml), BDNF (20 ng/ml), and Wnt3a (20 ng/ml). Wnt3A was removed from the medium.

Measurements were performed on these neurons approximately 4.5 weeks after the start of the differentiation date, which is about a week later than the measurement in our previous study denoted as t* (1). This 4.5-week time point is denoted throughout the manuscript as t2; an earlier time point of around 2.5 weeks is denoted as t1.

Cell culture: CA3 neurons

Briefly the same protocol was used as for culturing DG neurons; the only change was in the concentration of Wnt3A to 5 ng/ml. Neurons were measured at t1 (2.5 weeks) and t2 (4 weeks).

Cell culture: motor neurons

Briefly, iPSC colonies were grown in TeSR until confluency of 80%. They were dissociated using collagenase IV for 10 minutes to form EBs. Floating EBs were kept in TeSR +Rock inhibitor suspension for one day and TeSR for one more day. At day 2, we started the induction with DMEM/F12 +N2+ B27 with RA +Retinoic acid (1uM). At day 9, SHH (200 ng/ml) was added to the induction medium. EBs were kept in suspension for 25 days in total. On day 25 the EBs were dissociated with papain/DNase for 45 minutes and plated onto laminin/poly-L-ornithin-coated coverslips in neural induction medium consisting of DMEM/F12, N2 supplement, B27, BDNF, GDNF and Laminin. After 3-4 weeks neurons were infected with HB9::GFP lentivirus. After 7–8 days in culture in the coverslips, a feeder layer of spinal astrocytes (human Astrocytes-spinal cord (HA-sp) Catalog #1820, ScienCell Research Laboratories) was plated on

top of the neurons. The medium was changed to a differentiation medium consisting of neurobasal medium, N2 supplement, B27 with RA, retinoic acid (1 mM), cAMP (1 mM), and BDNF, GDNF, and laminin (all at 10 ng/ml), and 2% FBS. The neurons were cultured in the differentiation medium for about 2 more weeks before patch clamp experiments.

Analysis of electrophysiological recordings

Signals were amplified with aMulticlamp700B amplifier and recorded with Clampex 10.2 software (Axon Instruments). Data were acquired at a sampling rate of 20 kHz and analyzed using Clampfit-10 and the software package Matlab (2014b, The MathWorks Inc., Natick, MA, 2000). Neurons patched at room temperature and were generally with the brighter GFP signal, large (as is customary in the field (2)), and with a neuronal morphology.

Total evoked action potentials

Similar to our previous study (1), cells were typically held in current clamp mode near -60 mV with a steady holding current, and current injections were given starting 5 pA below the steady holding current, in 3 pA steps of 400 ms in duration. A total of 35 depolarization steps were given. Neurons that needed a current injection of more than 50 pA to be held at -60 mV were discarded from the analysis. The total number of action potentials was counted in 35 depolarization steps, starting from the first depolarization step, which was 10 pA below the current and caused the membrane potential to be at -60 mV (typically around 0). This total number of evoked potentials was used as an excitability measure throughout the study.

Spontaneous activity

The spontaneous activity (rate and amplitude) was measured in voltage clamp mode, holding the cell at a potential of around -45 mV.

Spike shape analysis

The first evoked action potential was used for spike shape analysis (with the lowest injected current needed for eliciting an action potential). Spike threshold was the membrane potential at which the slope of the depolarizing membrane potential increased drastically, resulting in an action potential (the first maximum in the second derivative of the voltage vs. time). The 5-ms AHP amplitude was calculated as the difference between the threshold for spiking and the value of the membrane potential 5 ms after the potential returned to cross the threshold value at the end of the action potential. The spike amplitude was calculated as the difference between the maximum membrane potential during a spike and the threshold. Action potential width was calculated as the time it took the membrane potential to reach half the spike amplitude in the rising part of the spike to the descending part of the spike (Full Width at Half Maximum).

Input conductance

The input conductance was calculated around the resting membrane potential by measuring the current with the cell held in voltage clamp mode first at -70 mV and then at -50 mV. The difference in currents divided by the difference in membrane potential (of 20 mV) is the calculated input conductance.

Sodium and potassium currents

The sodium and potassium currents were acquired in voltage clamp mode. Cells were held at −60 mV, and voltage steps of 400 ms were made in the range of −90 mV to 80 mV. Normalized currents are given by dividing the currents by the cell capacitance (changing the units from pA to pA/pF), by an automatic Matlab script. The capacitance was measured using the membrane test in Clampex SW.

Sodium currents

The amplitude of the sodium currents was calculated as the amplitude of the inward currents in voltage clamp mode in different test potentials. Immediately after a depolarization step, there is a strong capacitive transient that interferes with the measurements (see Fig. 2P; the transient current is circled in black). To eliminate these currents, we assumed that, to a close approximation, the membrane in voltage clamp behaves as a resistor and a capacitor in a parallel electrical configuration. During a voltage step, the current in the capacitor behaves approximately as the derivative of the change in potential (I=C*dVc/dt) and is therefore much stronger during fast transients than the currents going through the resistor. Therefore, for fast transitions in the membrane potential, we can assume a capacitive impedance that scales close to linearly with the voltage step (dVc). We therefore measured the current with a -10 mV voltage step from -60 mV to -70 mV, where there are no voltage gated channels that are open, and we used this as the reference capacitive current. We then scaled this linearly with the voltage step (i.e., for a 20 mV voltage step we would multiply the current produced by the -10 mV step by -2), and subtracted with the measurement performed to eliminate almost completely the capacitive transient current (see Supplementary Fig. S10 for an example). This estimation did not hold very well for test potentials above 30 mV, and therefore we show the sodium currents in the range of -80 mV to 20 mV, which account for physiological conditions. It is also important to note that our measurements of sodium currents may contain a mixture of somatic and axonal sodium currents. Milescu et al. (3) have shown that the axonal sodium currents may cause a skew in the measurements for depolarization potentials that are less than -20 mV. Therefore, throughout the study we will assume that the measurements are correct to a good approximation in the -20 mV to 20 mV depolarization range.

Slow potassium currents

The slow potassium currents were acquired in voltage clamp mode. Cells were held at −60 mV, and voltage steps of 400 ms were made in the range of −90 mV to 80 mV. The slow potassium currents were calculated by averaging the outward current over 50 ms starting 300 ms after the depolarization step using an automated Matlab script. The extrapolated currents arising from channels that are open at -60 mV (such as the inward rectifying potassium channels) were subtracted from this current. For normalized currents, the current that was calculated was divided by the capacitance measured using the membrane test of Clampex (changing the units to pA/pF). In addition, we calculated the currents manually in the 0 mV and 20 mV test potentials, where there were fluctuations of the currents due to sodium channels that opened when the voltage patch was not perfect. We manually calculated the potassium currents in these test potentials, avoiding these fluctuations (which an automated script cannot do properly) (see example of the fluctuating currents in Supplementary Fig. S6A with an expansion of the -20 mV depolarization in Supplementary Fig. S6B. It is clear that an automated script would have not been able to correctly calculate the slow potassium currents due to these fluctuations, and therefore a manual approach was substituted in the -20 mV – 0 mV depolarization steps).

Fast potassium currents

We measured the fast potassium current by the peak current following a depolarization step, typically within a time window of a few milliseconds, using an automated Matlab script that searched for the maximum current within a window of 70 ms after the depolarization step. The extrapolated currents arising from channels that are open at -60 mV (such as the inward rectifying potassium channels) were subtracted from this current.

Excitability graph as a radius of the dot

To visualize excitability of the neurons as a circle whose radius represents excitability, we used the following formula: $r = total\ number\ evoked\ potentials^{0.85}$. The 0.85 exponentials was used just for visualization purposes. Generally, larger circles represent more excitable neurons.

Kinetics of inactivation of fast potassium currents

An exponential decay coefficient was fitted to the decay of the fast potassium current from the maximum outward current at different depolarization steps to the current at 200 ms after the voltage step. This decay coefficient was considered the kinetics time constant of the inactivation or the fast potassium currents.

Activation kinetics of potassium currents

This was calculated as the time it took the outward current to reach 87% ($0.87=1-e^{-2}$) of the maximum outward current that was achieved within 8 msec of the depolarizing potential step. Since the current behaves approximately as

$I_f * (1 - e^{\frac{-t}{tau}})$, I_f being the value reached after a long time, then measuring at 87% of the final value corresponds to 2 times the time constant of the activation of the potassium currents.

Imaging of soma size

During electrophysiological recordings, the images of the neurons recorded were captured for later analysis of the soma size, which was done using ImageJ SW.

Tracing of neural progenitor cells (NPCs)

NPCs were plated on glass coverslips and fixed 24 hours after plating using 4% paraformaldehyde (PFA). Thirty cells were then imaged from each group and analyzed with Neurolucida SW, where neurites and soma were manually traced.

Immunohistochemistry

Cells were fixed in 4% paraformaldehyde for 15 minutes. Cells were subsequently blocked and permeabilized in PBS containing 0.1%–0.2% triton X-100 and 10% horse serum. Coverslips were incubated with primary antibody in blocking solution overnight at 4°C, washed in Tris-buffered saline, incubated with secondary antibodies for 30 minutes at room temperature, counterstained with DAPI, washed, mounted on slides using PVA-DABCO (Sigma-Aldrich), and dried overnight protected from light. The following antibodies and dilutions were used: Map2ab (1:1000), ELAVL2 (1:250), ELAVL2/4 (1:500), NeuN (mouse, 1:100, Millipore), ELAVL2 (1:100), and GABA (1:1000), Islet (1:250, Cat # 39.4D5, Developmental Studies Hybridoma Bank). Fluorescence signals were detected using a Zeiss 710 confocal microscope and images were processed with Zen and ImageJ.

It is important to note that, in our cultures, we see a similar distribution of 10-15% GABAergic neurons and 85-90% glutamatergic neurons as previously described using these protocols (4, 5). iPSC-derived neuronal cultures generally display mostly glutamatergic neurons as well as other neuronal types and astrocytes (6). The developmental aspects of the types of cells found are described in (7). This study will be focusing on the physiology of the neurons in the culture that are marked with specific reporters such as prox1 (DG) and ELAVL2 (CA3).

RNA preparation and qPCR: CA3 neurons

Total cellular RNA was extracted from 3-5 million cells per sample at 30 days post-differentiation using the RNA-BEE (QIAGEN) (see Supplemental Methods) according to the instructions supplied with the kit, and then reverse transcribed using the high-capacity cDNA synthesis kit from AB Biosystems. qPCR was done using SYBR green (Life Technologies). Samples with cycle threshold (CT) values of more than 30 were discarded from the analysis. qPCR results were analyzed using SDS Software v 3.2 for a 7900HT real-time PCR system.

Supplementary results

DG compared to CA3 neurons

Generally, CA3 neurons of the control and LR groups produced more action potentials than DG control and LR groups (at the same age of the neurons), respectively, but CA3 NR neurons did not produce more action potentials than NR DG neurons (Supplementary Fig. S3A). It was previously reported that DG granule neurons are inactive compared to other neuronal types in the hippocampus (8), and this may be the reason that in our experiments control and LR DG neurons are less excitable than control and LR CA3 neurons. In addition, CA3 neurons are larger in size, and therefore can sustain higher current injection before sodium channels inactivate. Supplementary Figures S3B-S3C show the number of evoked potentials at an earlier time point (t1=14-23 days after start of differentiation, with an average time point of 2.5 weeks; see Methods), and Supplementary Figure S3F shows the development over time of the excitability (total evoked potentials) for DG and CA3 neurons. At t1, DG neurons already exhibited differences between the 3 groups, whereas in CA3 neurons the differences were not yet evident (Supplementary Fig. S3B). There was no significant difference between the spontaneous activity of DG and CA3 neurons in any of the 3 groups (Supplementary Fig. S3D for rate, and S3E for amplitude).

Neural progenitor cells (NPCs), CA3 pyramidal and DG granule neurons are larger when derived from BD patients than from controls

In our previous study (1), we reported that DG neurons derived from BD patients were larger 3.5 weeks after starting differentiation from NPCs; specifically, the NR group neurons were the largest. We measured the capacitance of CA3 pyramidal neurons at t2=4.5 weeks (Supplementary Fig. S8A) and similarly observed that BD neurons were larger than controls and the NR group neurons were the largest (~30% increase in capacitance for the LR group, and 70% increase for the NR group when compared to the control group). The development course of the capacitance is shown in Supplementary Figure S8B. Imaging of the soma and tracing its size using ImageJ SW showed similar increases in cell size (Supplementary Fig. S8C). The ratio of capacitance to soma size was similar between the 3 groups (Supplementary Fig. S8D), indicating that there was a similar increase in neurite length and that the changes to the cell size in BD were scaled similarly throughout the entire cell. Example images of control, LR and NR CA3 neurons are provided in Supplementary Figure S7E-G. We were interested to see if these differences manifested as early as the NPC stage, so we imaged 75 control NPCs from the 4 patients, 60 LR NPCs (3 patients) and 60 NR NPCs (3 patients) and measured the soma size and the total neurite tree length. Interestingly, the soma was already larger in LR NPCs compared to controls, and even larger in NR NPCs (Supplementary Fig. S7H). The total neurite length was larger in the NR NPCs than in the controls (Supplementary Fig. S7I). Examples of control, LR and NR NPC images are shown in Supplementary Figure S7J-L.

Overexpression of the Kcnc genes in our previously published cohort in LR neurons

After observing these changes in expression of the Kcnc genes in the CA3 neurons from this cohort, we re-analyzed our already published data (9) and separated the previously reported cohort into 3 groups - control, LR and NR - to look at expression differences in the Kcnc genes. The results are plotted in Supplementary Figure S4. An overexpression of the Kcnc2 gene was observed in LR neurons. A similar overexpression of Kcnc3 was observed in LR neurons and a reduced expression in this gene was observed in the NR neurons. These Kcnc genes belong to a family of rapidly activating and deactivating potassium channels, allowing for high frequency firing like we see in the LR hippocampal neurons (10, 11).

Lithium increases sodium currents but reduces the amplitude of the fast potassium currents, resulting in a reduction of hyperexcitability of neurons derived from BD patients who respond to lithium (LR)

We were interested to see which of the test potentials produced currents that correlated most with excitability (in continuation with the plots presented in Fig. 3C-H). We calculated the correlation of the cell excitability (as measured by the total amount of evoked potentials) and a few of the features and currents that were measured. The excitability generally correlated with capacitance for control and LR neurons (Supp. Fig. S8A-B), whereas it did not correlate with capacitance in NR neurons (Supp. Fig. S8C). This miscorrelation of excitability with capacitance specifically in NR neurons was previously reported in our study with DG neurons (1). In LR neurons, where we have seen that lithium treatment reduced capacitance, the correlation grew stronger between excitability and capacitance after lithium treatment. Only in NR untreated neurons did the excitability correlate with the slow potassium currents (at 10 mV, Supp. Fig. S8D-F). In LR and NR neurons, the excitability correlated much more strongly with the fast potassium currents at the lower depolarization steps (Supp. Fig. S8G-I) than with the fast potassium currents at the higher depolarization steps (Supp. Fig. S8J-L). And finally, as expected, the excitability correlated with the amplitude of the sodium currents (at -20 mV). The very strong correlation specifically for the NR neurons ($R=0.73$, $p=6e-12$) and the large slope of the line representing excitability as a function of sodium currents in NR neurons were notable (Supp. Fig. S8M-O).

To summarize, lithium affected the cells in several ways. It reduced the huge capacitance of BD neurons. It increased the amplitude of the sodium currents in all 3 groups, and it reduced the amplitude of the fast potassium currents at the lower depolarization holding potential in the LR group (currents that we have showed correlate with excitability). We therefore think that this may be lithium's dual way of operation as a mood stabilizer: increasing sodium currents and thus reducing the amount of hypoexcitable cells on one hand, but also reducing the fast potassium currents and thus reducing the total number of hyperexcitable cells.

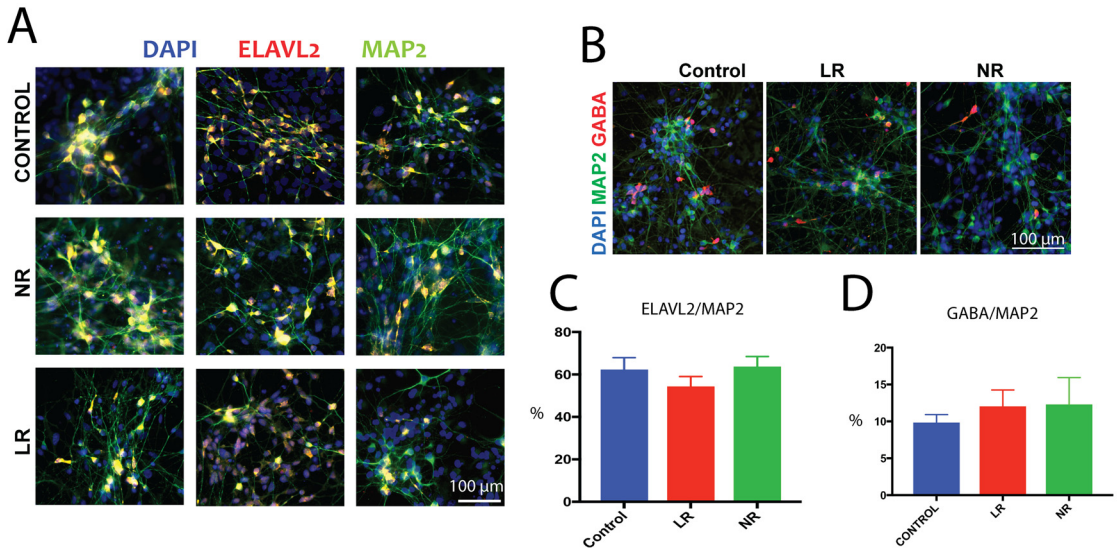

Supplementary Figure S1. Neuronal markers and potassium channels expression. A. Example images of immunostaining for 4′,6-diamidino-2-phenylindole (DAPI, blue, marks the nucleus), ELAV-like RNA binding protein 2 (ELAVL2, red, specific marker of CA3 pyramidal neurons) and microtubule associated protein 2 (MAP2, green, enriched in neurites). B. Example images of immunostaining for GABA-expressing neurons in control neurons, LR and NR cultures. C. Percentage of ELAVL2 and MAP2-expressing neurons is approximately 60% of all the MAP2 expressing neurons in all 3 groups, indicating that our differentiation protocol is efficient. D. No significant change between the 3 groups in the percentage of GABA and MAP2-positive neurons (ranging 10-13% out of all the MAP2 expressing neurons).

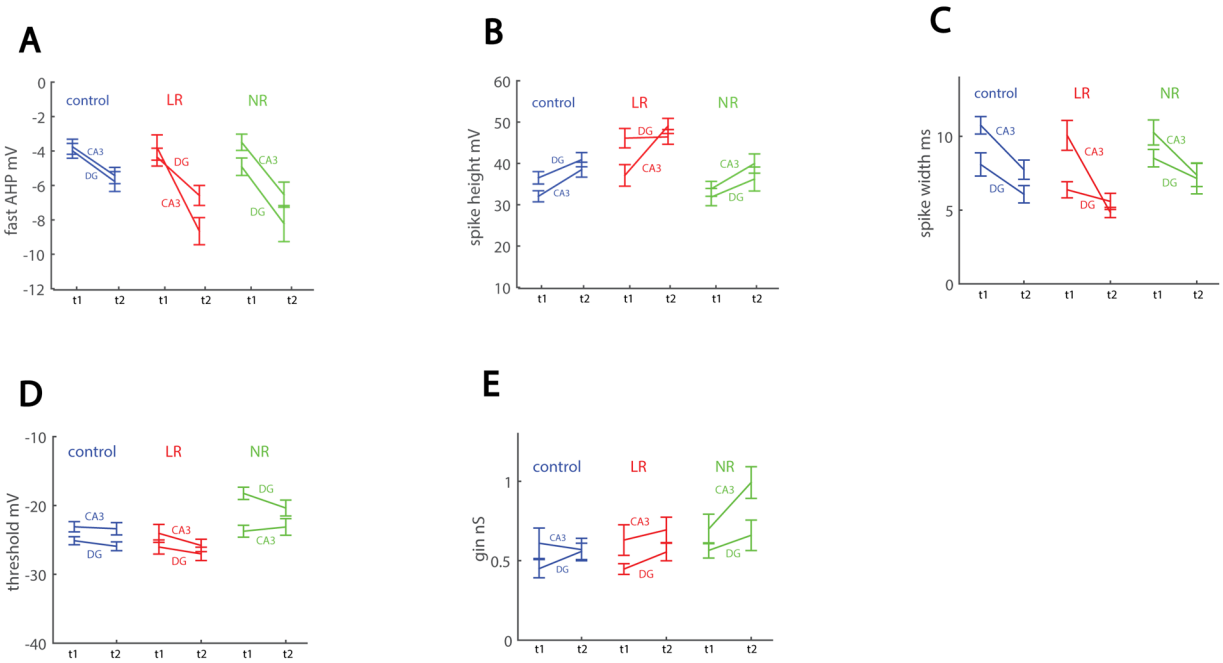

Supplementary Figure S2. Development over time of spike shape features. Development from t1 to t2 of the A. fast AHP, B. spike height, C. spike width, D. threshold for evoking an action potential and E. input conductance in DG and CA3 neurons for the 3 groups: control, BD LR, and BD NR.

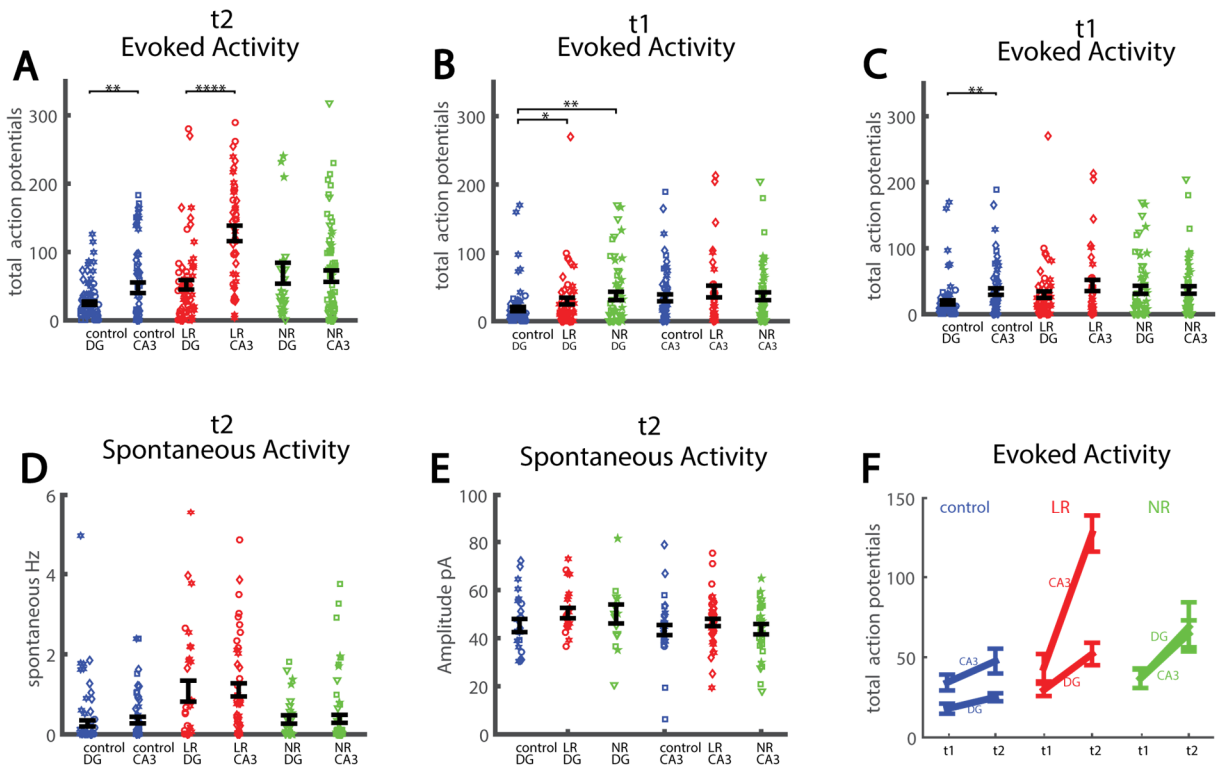

Supplementary Figure S3. Each dot in this figure represents one cell. The different human subjects are marked with a different shape of the dot. A. Comparison of excitability between DG and CA3. CA3 neurons produce more evoked potentials in the control and LR groups. In the NR group there is a similar number of evoked potentials between DG and CA3 neurons. B. Excitability at t1 (2.5 weeks). There is a significant increase in excitability in the NR and LR groups in DG neurons compared to controls, but no change in CA3 neurons between the 3 groups. This indicates that the differences between BD and control in the DG neurons appear before the differences in the CA3 neurons C. Excitability comparison between DG and CA3 neurons at t1=2.5 weeks. CA3 control neurons produce more evoked potentials than DG neurons. D. Comparison of spontaneous activity rate between DG and CA3 neurons at t2=30 days reveals similar spontaneous activity rate between DG and CA3 neurons in all 3 groups. E. No changes are observed in the spontaneous spike amplitude between the 3 groups in both DG and CA3 neurons. F. Development over the time period between t1 and t2 of neuronal excitability (total evoked action potentials) of DG and CA3 neurons of the 3 groups: control, LR and NR. Asterisks represent statistical significance by the following code: * p value<0.05, **p value<0.01, ****p<0.0001. Error bars represent standard error.

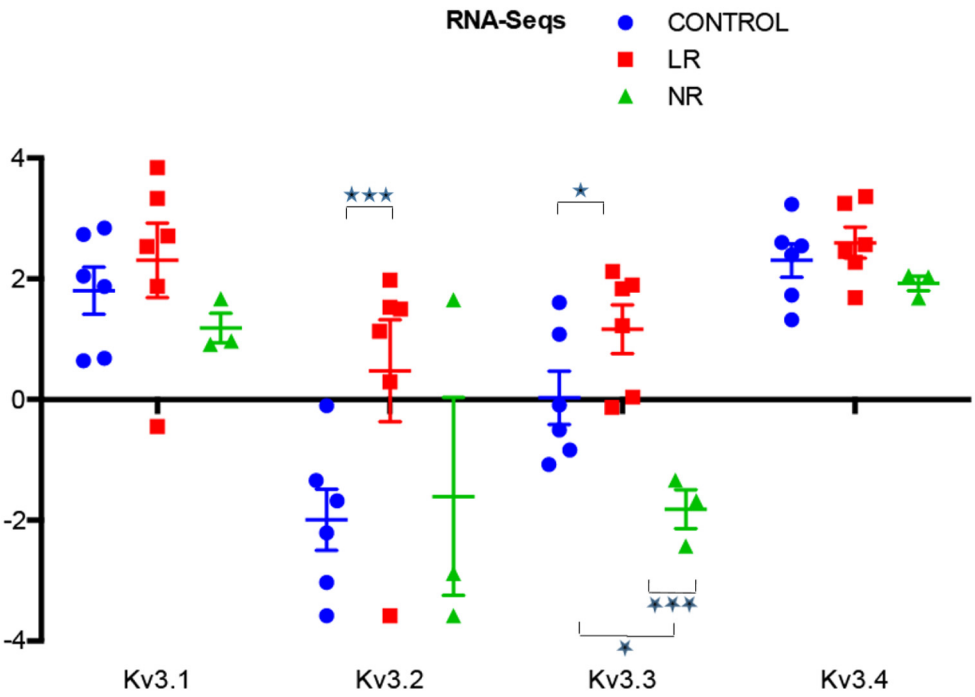

Supplementary Figure S4. Fpkm values of RNA sequencing from DG neurons derived from our previous cohort (9). Similar to CA3 neurons derived from the current cohort, LR neurons have an overexpression of Kcnc2 and Kcnc3 potassium channels whereas NR neurons have a decreased expression of Kcnc3 expression.

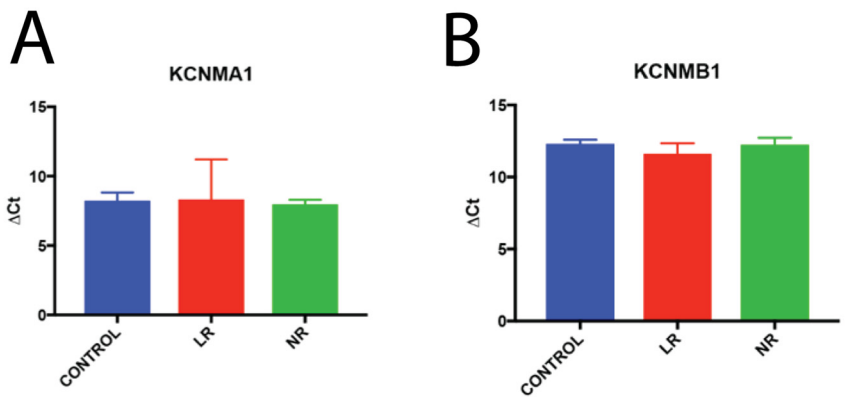

Supplementary Figure S5. qPCR of KCNMA1, KCNMB1. A. No significant change in expression of KCNMA1 gene between the 3 groups. B. No significant change in expression of KCNMB1 gene in the 3 groups.

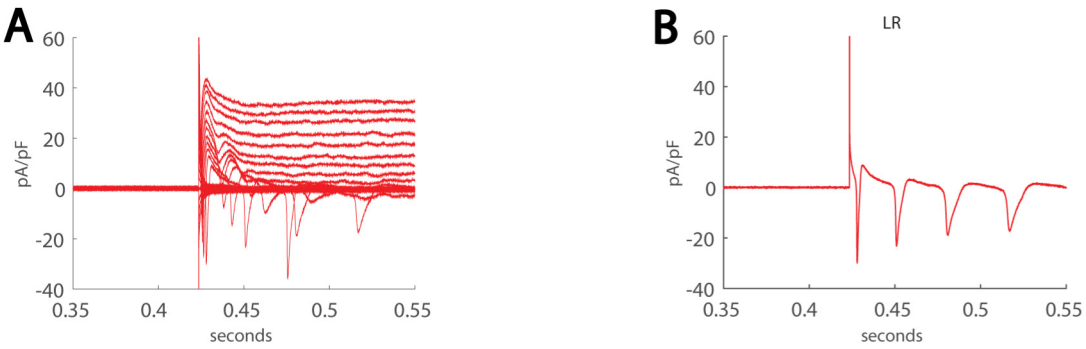

Supplementary Figure S6. An example recording in voltage clamp mode demonstrating fluctuations of the currents at low depolarization steps (around 0 mV). A. Due to fluctuations in the currents, the potassium current should be calculated manually at the low (-20 mV – 20 mV) depolarization steps. B. The trace at a depolarization step of -20 mV demonstrates the fluctuations in the current due to opening of sodium currents. Clearly from this trace, an automated script would not calculate the slow potassium current correctly, and therefore we employed a manual approach for the -20 mV – 20 mV depolarization steps.

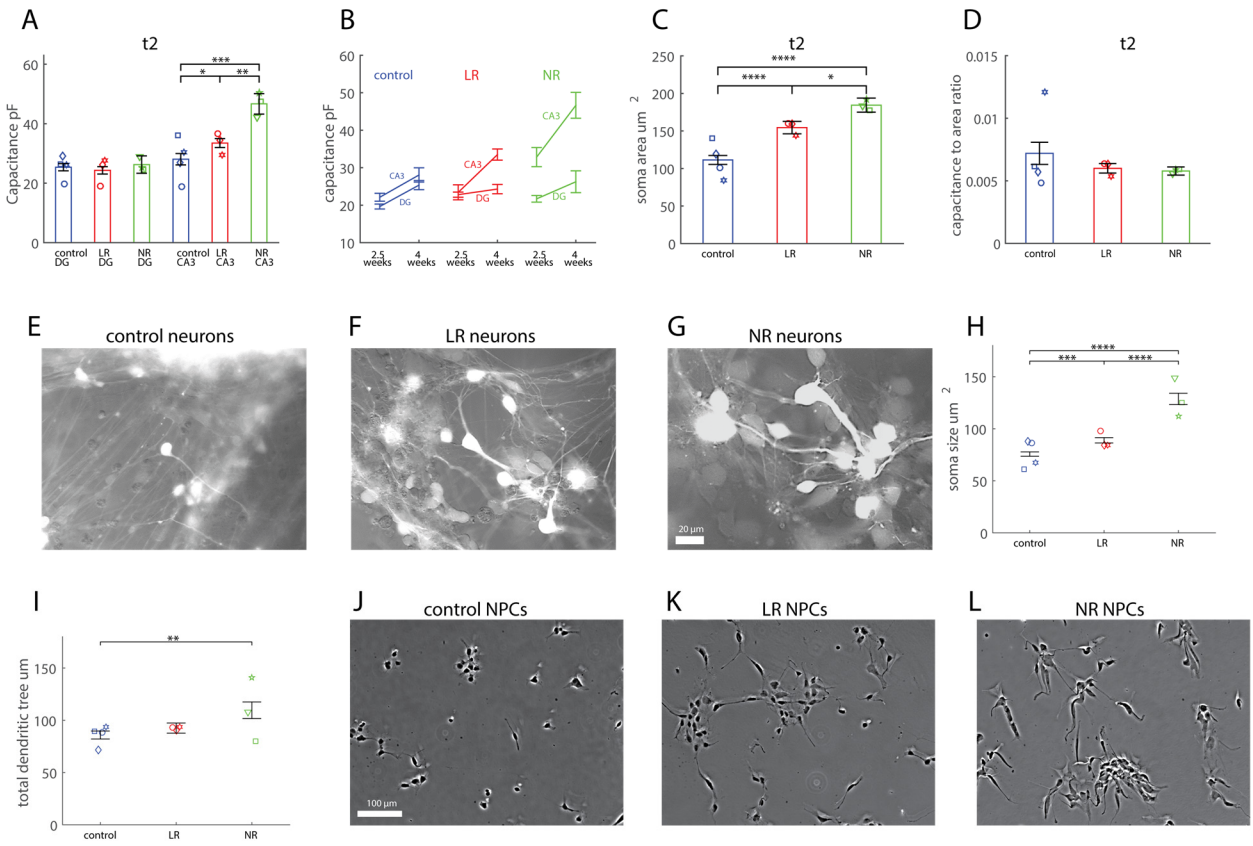

Supplementary Figure S7. BD neurons and NPCs are larger than controls. A. The capacitance of CA3 BD LR neurons is larger than the controls' capacitance, and CA3 NR neurons are even larger (around 70% increase compared to controls). [Remark: In our previous report, at around 25 days, BD DG neurons were larger than controls as well (1)] B. Development from t1=2.5 weeks to t2=30 days. C. Imaging of the soma of CA3 neurons further supports the capacitance changes: soma is larger for CA3 LR neurons and even more for CA3 NR neurons. D. The ratio of capacitance to soma size is not changed between the groups - control, BD LR and BD NR - indicating that there are similar larger neurites in LR BD and even more in NR BD compared to controls. E. Example of a control soma. F. Example of a BD LR soma. G. Example of a BD NR soma. H. Imaging of a total of n=30 from each patient of neural progenitor cells (NPCs) further shows that there is a change in cell size as early as the NPC stage (each dot in the graph represents the average of one human subject). I. The initial neurites at the NPC stage are larger in BD NR neurons. J. A representative image of control NPCs. K. A representative image of BD LR NPCs. L. A representative image of BD NR NPCs. Asterisks represent statistical significance by the following code: * p value<0.05, **p value<0.01, ***p<0.001, ****p<0.0001. Error bars represent standard error.

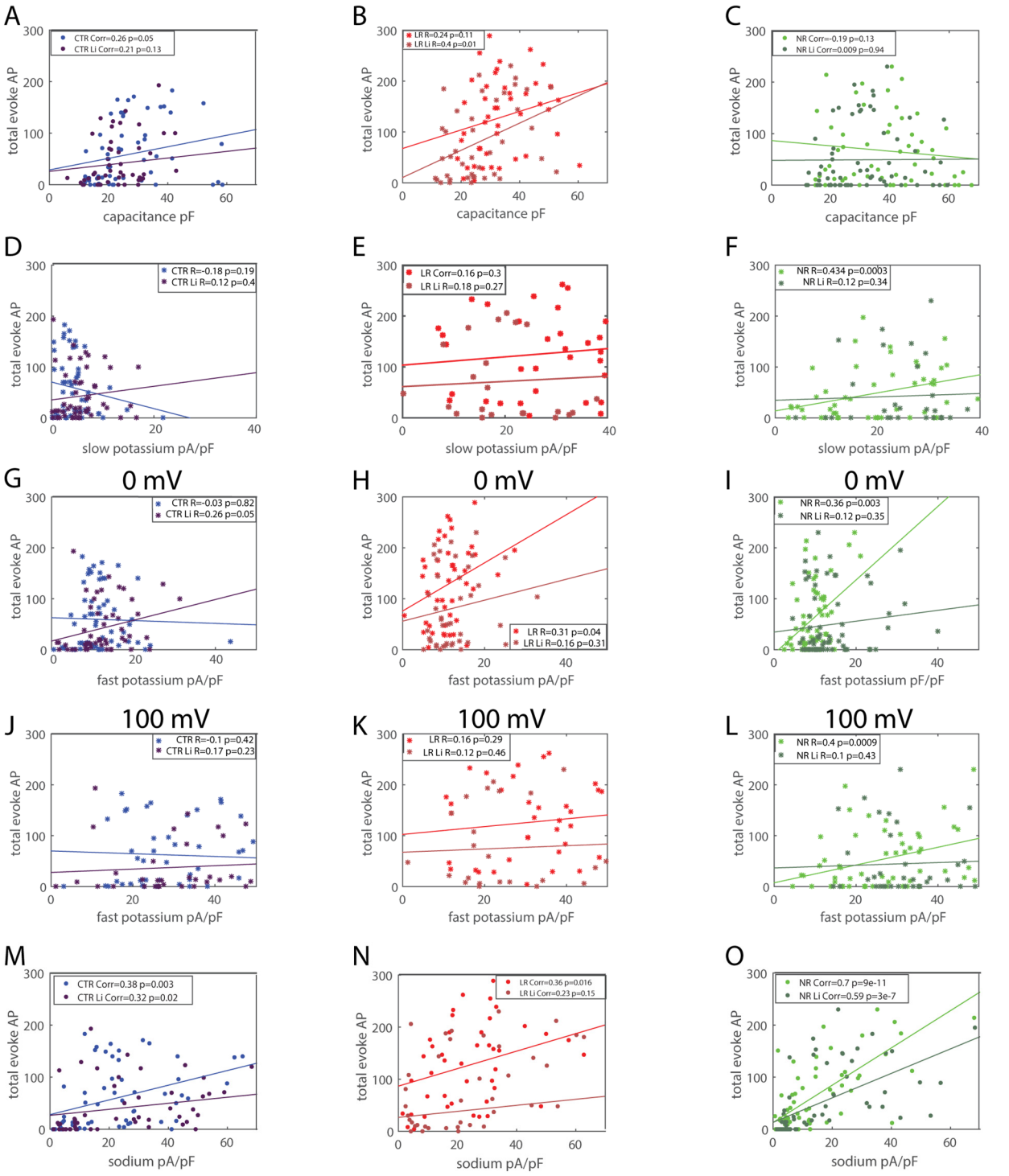

Supplementary Figure S8. Correlations of CA3 excitability with currents at t2=30 days. A-C. Control and LR excitability correlates significantly with cell capacitance, but this correlation is completely lost in NR neurons. D-F. Control and LR neurons weakly correlate with the amplitude of the slow potassium currents at 10 mV, but a significant correlation is observed in NR neurons (which diminishes with lithium treatment). G-I. A strong correlation is observed between excitability and the amplitude of the fast potassium currents at 0 mV in LR and NR neurons. This correlation weakens with lithium treatment. Control neurons'

excitability does not correlate with the amplitude of the fast potassium currents at 0 mV, but this correlation is seen with lithium treatment. J-L. Control and LR excitability does not correlate with the amplitude of the fast potassium current at 100 mV. However, NR excitability does correlate with the amplitude of the fast potassium current at 100 mV. This correlation diminishes after lithium treatment. M-O. All the groups correlate with sodium currents (at -20 mV). This correlation is much stronger in NR neurons compared to control and LR neurons, and so is the incline of the graph. This correlation weakens a bit with lithium treatment but remains very significant.

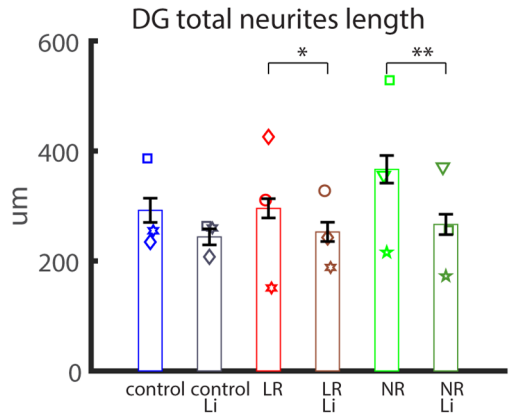

Supplementary Figure S9. Chronic lithium treatment in DG neurons reduces the total length of the dendritic tree in the three groups (control, LR and NR), with a significant effect in the BD neurons. Asterisks represent statistical significance by the following code: * p value<0.05, **p value<0.01

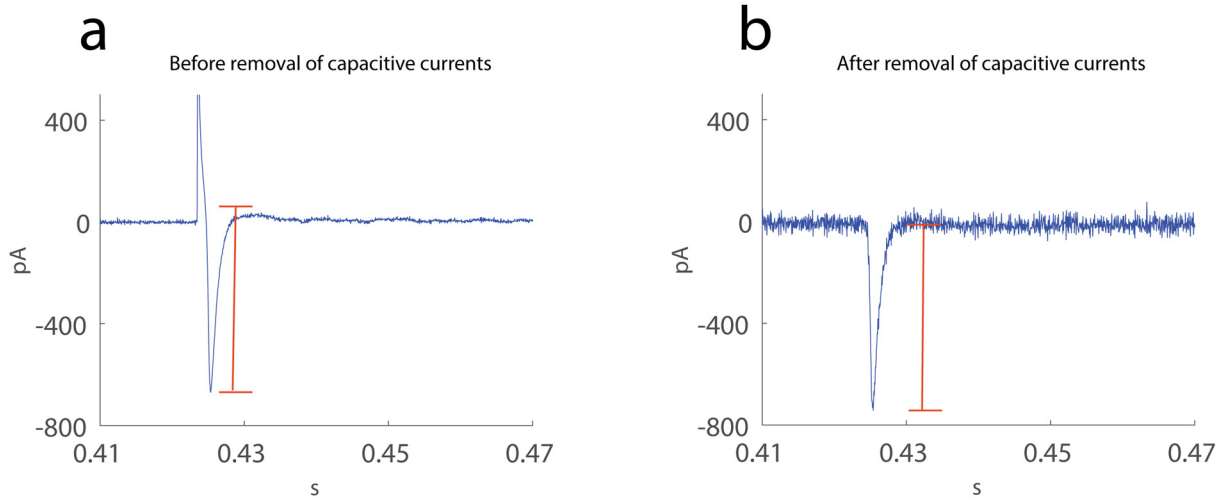

Supplementary Figure 10. A demonstration of the measured sodium currents. A. Example trace of currents in voltage clamp mode demonstrates how the strong transient capacitive currents disrupt the measurement of the sodium currents. The red line demonstrates the sodium current that should be measured. B. A compensation for the capacitive current (see Supplementary methods) allows for measurement of the sodium current in different depolarization steps. In red is the sodium current that is calculated by an automated Matlab script after the compensation for the capacitive current.

Supplementary Table S1

Cell ID	Catego	Age	Age at onset	Diagnosis	Sex	Ethnicity	Episodes off Li*	Episodes on Li*	Years on Li at sampling	Response score**	SCC code
21868	R	50	31	BPI	M	Caucasian	3M 4D	0	5	9/10	SBP010
35794	R	41	34	BPI	M	Caucasian	5M 1D	0	3	10/10	SBP005
7762	R	34	15	BPI	M	Caucasian	3M 1D	0	4	9/10	SBP007
24339	NR	51	35	BPI	M	Caucasian	1M 1D	1M	2	3/10	SBP001
20026	NR	58	22	BPI	M	Caucasian	3M 5D	2D 1RC	6	1/10	SBP002
14501	NR	40	24	BPI	M	Caucasian	4M 3D	7M	7	0/10	SBP004
37014	C	62	n/a	n/a	M	Caucasian	n/a	n/a	n/a	n/a	SBP011
31616	C	25	n/a	n/a	M	Caucasian	n/a	n/a	n/a	n/a	SBP008
40064	C	51	n/a	n/a	M	Caucasian	n/a	n/a	n/a	n/a	SBP009
7158	C	53	n/a	n/a	M	Caucasian	n/a	n/a	n/a	n/a	SBP012

* D = major depression; M = mania; RC = period of rapid cycling

** Reference (12)

Supplemental References

1. Stern S, Santos R, Marchetto MC, Mendes APD, Rouleau GA, Biesmans S, et al. (2018): Neurons derived from patients with bipolar disorder divide into intrinsically different sub-populations of neurons, predicting the patients' responsiveness to lithium. *Mol Psychiatry*. 23:1453-1465.
2. Stern S, Segal M, Moses E (2015): Involvement of Potassium and Cation Channels in Hippocampal Abnormalities of Embryonic Ts65Dn and Tc1 Trisomic Mice. *EBioMedicine*. 2:1048-1062.
3. Milescu LS, Bean BP, Smith JC (2010): Isolation of somatic Na+ currents by selective inactivation of axonal channels with a voltage prepulse. *J Neurosci*. 30:7740-7748.
4. Yu DX, Di Giorgio FP, Yao J, Marchetto MC, Brennand K, Wright R, et al. (2014): Modeling hippocampal neurogenesis using human pluripotent stem cells. *Stem cell reports*. 2:295-310.
5. Sarkar A, Mei A, Paquola ACM, Stern S, Bardy C, Klug JR, et al. (2018): Efficient Generation of CA3 Neurons from Human Pluripotent Stem Cells Enables Modeling of Hippocampal Connectivity In Vitro. *Cell Stem Cell*. 22:684-697 e689.
6. Kang S, Chen X, Gong S, Yu P, Yau S, Su Z, et al. (2017): Characteristic analyses of a neural differentiation model from iPSC-derived neuron according to morphology, physiology, and global gene expression pattern. *Sci Rep*. 7:12233.
7. Hu BY, Weick JP, Yu J, Ma LX, Zhang XQ, Thomson JA, et al. (2010): Neural differentiation of human induced pluripotent stem cells follows developmental principles but with variable potency. *Proceedings of the National Academy of Sciences of the United States of America*. 107:4335-4340.
8. Senzai Y, Buzsaki G (2017): Physiological Properties and Behavioral Correlates of Hippocampal Granule Cells and Mossy Cells. *Neuron*. 93:691-704 e695.
9. Mertens J, Wang QW, Kim Y, Yu DX, Pham S, Yang B, et al. (2015): Differential responses to lithium in hyperexcitable neurons from patients with bipolar disorder. *Nature*. 527:95-99.
10. Hurlock EC, Bose M, Pierce G, Joho RH (2009): Rescue of motor coordination by Purkinje cell-targeted restoration of Kv3.3 channels in Kcnc3-null mice requires Kcnc1. *The Journal of neuroscience : the official journal of the Society for Neuroscience*. 29:15735-15744.
11. Kaczmarek LK, Zhang Y (2017): Kv3 Channels: Enablers of Rapid Firing, Neurotransmitter Release, and Neuronal Endurance. *Physiol Rev*. 97:1431-1468.
12. Grof P DA, Cavazzoni P, Grof E, Garnham J, MacDougall M, O'Donovan C, Alda M. (2002): Is response to prophylactic lithium a familial trait? . *The Journal of clinical psychiatry*. 63:942-947.